

# Empirical modeling of plasma clouds produced by the Metal Oxide Space Clouds (MOSC) experiment

Todd R. Pedersen<sup>1</sup>, Ronald Caton<sup>1</sup>, Daniel Miller<sup>1,3</sup>, Jeffrey M. Holmes<sup>1</sup>, and Keith M. Groves<sup>2</sup>

<sup>1</sup>Air Force Research Laboratory, Space Vehicles Directorate  
3550 Aberdeen Ave. SE  
Kirtland AFB, NM 87117  
United States of America

<sup>1</sup>Boston College, Institute for Space Research  
Chestnut Hill, MA  
United States of America

<sup>3</sup>No longer at AFRL

## ABSTRACT

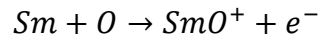
The Air Force Research Laboratory (AFRL) Metal Oxide Space Clouds (MOSC) experiment consisted of 2 upper atmospheric releases of samarium (Sm) from Kwajalein Atoll in the Marshall Islands in May 2013. The MOSC chemical release experiments employed the ALTAIR radar as a primary measurement of plasma density in the clouds. However, the radar provides only the local plasma density in the beam location, and the measurements are of limited value without context to determine the location of the radar beam relative to the larger plasma cloud. We have constructed an empirical model of the cloud locations, shapes, and sizes as a function of time for the MOSC launches using fits to all-sky images recorded from near the launch site. When combined with ALTAIR radar measurements of local plasma density at the sampled point and ionosonde measurements of the peak plasma density, a robust 4-D representation of the plasma density can be derived and used to study impacts on the background ionosphere and RF propagation.

## 1. INTRODUCTION

The Metal Oxide Space Clouds (MOSC) experiment consisted of 2 Terrier-Orion sounding rockets launched from the island of Roi Namur (9.4° N 167.5° E), part of Kwajalein Atoll in the Marshall Islands. The first rocket, which we shall refer to as Launch 1, was launched at 07:38:00 UT on 1 May 2013. The second flight, Launch 2, occurred at 07:23:00 UT on May 9, 2013. Both rockets carried identical payloads consisting of 2 chemical release canisters each containing approximately 3 kg of samarium (Sm) powder mixed with a titanium-boron (Ti-B) fuel in a pressure vessel. The canisters were triggered by an electrical signal to an explosive igniter, and the vaporized Sm was released ~1 sec later by rupture of a burst disk. The release from Launch 1 occurred at 159.9 seconds into the flight at an altitude of 171 km, while the Launch 2 release was at 177.6 seconds and 182 km altitude, on a nearly identical high-elevation trajectory. The launches were timed for evening twilight to provide sunlight at altitude and darkness on the ground to allow optical observations of cloud position, size, and spectra. The primary experiment diagnostics relevant to the present analysis were the ARPA Long-Range Tracking And Instrumentation Radar (ALTAIR) radar, used in incoherent scatter mode to measure electron densities in the artificial clouds and background

ionosphere, a DPS-4D ionospheric sounder system which can determine the maximum plasma frequency within the clouds, and an all-sky imager providing the intensity and spatial distribution of resonantly scattered optical emissions produced by solar illumination of the clouds. All three of these instruments were located on Roi Namur within 2 km of the launch site.

The primary objective of the MOSC experiments was to determine the potential to suppress the Rayleigh-Taylor instability responsible for nighttime ionospheric scintillation by creating enhanced conductivities on field lines threading the bottomside of the equatorial F-region. A secondary objective was to measure the direct effects of the artificial clouds on RF propagation. The presumed plasma production mechanism for the MOSC experiments was a chem-ionization or associative detachment reaction between the Sm vapor and atomic oxygen present in the background upper atmosphere:



Other ionization possibilities also exist, however, including direct photoionization of Sm, and photoionization of unreacted Ti from the canister.

Regardless of the ionization mechanism, achievement of both experiment objectives requires an accurate reconstruction of the actual location, shape, and density of the artificial plasma clouds from measurements. In particular, the ALTAIR radar has a narrow beam, and plasma density measurements within the beam only provide a minimum constraint on the possible range of plasma densities within the cloud, as there is no way of determining from the radar data alone where the sampled points lie relative to the rest of the cloud.

## 2. OBSERVATIONS

To capture the expected dynamic evolution of the clouds, the ionosonde made near-vertical-incidence frequency sweeps every 60 seconds during the launches. The optical imager cycled through 6 filter wheel settings each minute, capturing emissions over  $\sim 2$ nm bands at 630.0, 557.7, 427.8, 777.4, and 844.6 nm, at automatically adjusted exposure times up to 8 seconds. Additionally, a broadband unfiltered exposure was also taken each minute, but was generally overexposed in the central region of the clouds. Note that the filter wavelengths correspond to natural airglow and auroral emissions, and were not optimal for the Sm releases as reference spectra for the expected  $SmO^+$  ions were not available in the literature and filters of the appropriate size and passband for other less important species were prohibitively expensive. The ALTAIR radar was operated in continuous data collection mode from before the launch to several hours after the release. The radar was initially pointed at the azimuth and elevation predicted for the release, and programmed to then follow a raster scanning pattern that would provide the optimum likelihood of cutting across the clouds to provide plasma density profiles. The optical images were provided with azimuth and elevation overlays in real time and used to interactively reposition the radar as the clouds drifted away from the initial release position. This procedure was very effective during the second launch when optical positions were called in in real time from the imager location by telephone and clear density signatures were observed with the radar in real time, but was only marginally successful during the first launch when latency in data delivery from the imager to the radar control room and lack of obvious real-time signatures in the radar data combined with more dynamic background conditions to allow the cloud to escape radar coverage for much of the time.

The general evolution of the clouds can be described in qualitative terms as follows: the flash of the initial release was followed by the appearance of a rapidly expanding bluish-white spherical cloud, which after a minute or two began to change toward a more reddish color, with the red component stronger at the E side of the cloud and a blue component stronger toward the W. In Launch 1 the overall cloud elongated in the E-W direction at this point and began to move rapidly toward the W at a high enough rate to prevent successful repositioning of the radar to the new location. The cloud from Launch 2, by contrast, elongated slightly in the N-S (field aligned) direction and its drift motion gradually changed from SE to W and then NW. In both cases, all optical emissions disappeared after the terminator crossed the cloud altitudes and sunlight was no longer available to excite emissions. Neither cloud showed indications of small-scale structuring in any of the optical wavelengths or radio data, and optical intensities along cross-sections through the clouds were generally Gaussian at all wavelengths, although with noticeable asymmetries in gradients between the E and W sides of the clouds.

### 3. EMPIRICAL MODEL

The lack of small-scale structure and overall Gaussian character of the gradients led us to use a 2-D time-dependent Gaussian function to empirically describe the cloud over its lifetime. Individual image frames were extracted from the data and fit using the IDL Gaussfit\_2D procedure.

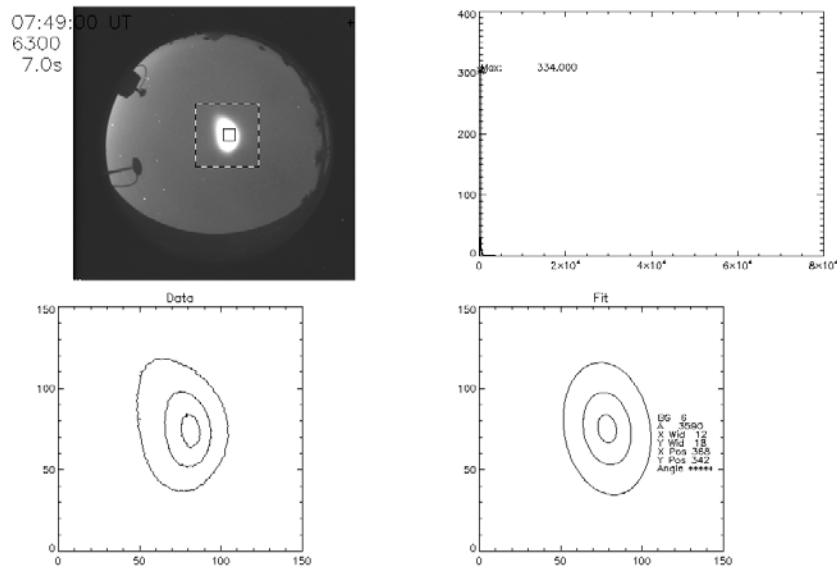


**Figure 1.** Raw optical all-sky image of the Launch 2 Sm cloud at 630.0 nm (upper left), background determination (upper right), contours of image intensity (lower left), and contours of the 2-D Gaussian fit to the (lower right).

This provided, for each image frame, in raw units of counts and pixels, the background intensity, peak cloud intensity,  $x$  and  $y$  positions,  $x$  and  $y$  widths, and tilt of the 2-D distribution relative to the  $x$  and  $y$  axes. The absolute background and cloud intensities are of minimal value to the analysis due to interference from ground lights and tropospheric clouds, not to mention the rapidly changing twilight illumination both on the ground and at altitude, but they do provide a solid indication of the quality of the data and consistency of the fits with time.

Successful optical fitting to a 2-D Gaussian led to formulation of the empirical model as a 2-D Gaussian spatial dependence scaled by a peak electron density:  $N(x, y, z, t) = N_0(t)e^{-\frac{u}{2}}$ , where  $u = \left(\frac{x'-x_0}{W_x}\right)^2 + \left(\frac{y'-y_0}{W_y}\right)^2 + \left(\frac{z-z_0}{W_z}\right)^2$  provides for Gaussian spatial dependence with characteristic sizes  $W$  in all 3 dimensions, and  $N_0(t)$  is the maximum plasma density in the cloud at any given time.  $x_0$  and  $y_0$  are empirical functions of time recovered from the fits to the image data, as are the characteristic sizes  $W_x$ , and  $W_y$ . The altitude dependence, which is not measurable without incorporating optical data from other sites, is assumed for this analysis to remain at the release altitude  $z_0$  and to have the same spatial structure as the E-W cross-field ( $x$ ) dependence for the width, i.e.  $W_z = W_x$ . The model allows for a rotation of the distribution about the vertical axis, such that  $x'$  and  $y'$  are in the rotated coordinates whereas  $x$  and  $y$  correspond to Cartesian coordinates in the eastward and northward directions, respectively. Although the fit parameters showed consistent differences between wavelengths, these were only a few pixels in magnitude and this initial version of the model represents the best fit across all observed wavelengths rather than a fit to a specific wavelength. In particular, the 427.8 nm images in the blue region of the spectrum show the clouds displaced slightly to the west relative to images in the red at 630.0 nm. Note that the present optics-based model formulation assumes that the actual plasma cloud corresponds in position and shape to the optical cloud, which may or may not be the case—it is entirely possible that all observed optical emissions come from neutral species and not ionized species. We will discuss the applicability of this assumption later.

### 3.1 CLOUD POSITION AND SIZE

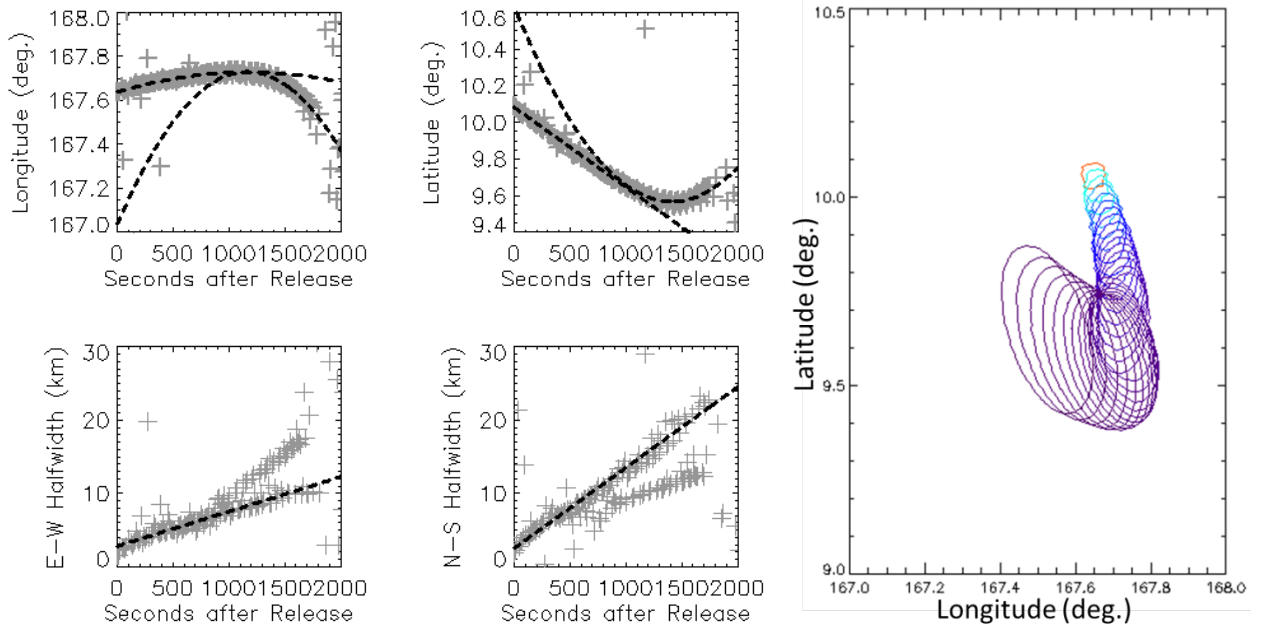


**Figure 2.** Cloud longitude and latitude fits (top left, top center) and half-widths (bottom left, bottom center) for Launch 2, along with contours of half-maximum as a function of time, latitude, and longitude (right) derived from the fits. Positions were converted from pixel coordinates to azimuth and elevation and then geographic coordinates based on the release altitude. The secondary sets of data points in the halfwidth plots are from the other axis with a  $90^\circ$  rotation of the coordinates, i.e. some of the fits swap the  $x$  and  $y$  axes but have a tilt  $90^\circ$  from the unaliased fits.

As mentioned, the optical cloud for Launch 2 moved gradually toward the SE, then toward the W and then NW. We were able to fit low-order polynomials piecewise to these positions for Launch 2 by breaking up the motion at 1000 sec after the release. The latitude dependence for Launch 2 is even simpler, being linear before 1000 seconds and parabolic after 1000 seconds.

Scale sizes (Gaussian half-widths)  $W_x$  and  $W_y$  are also straightforward to model, having a closely linear dependence over the entire time interval except the first minute or two after release when the cloud expanded at a much higher non-linear rate. For Launch 2 the N-S (field aligned) expansion rate was approximately twice as large as the E-W rate.

### 3.2 COMPARISON WITH DENSITY MEASUREMENTS

While the optical fits provide valuable measurements of the motion and expansion of the optical clouds, the intended objective is to describe the distribution of plasma density. As the optical measurements are inherently integrated along the near-vertical lines of sight, we first investigate the correlation between plasma density and the optical measurements by integrating the range-resolved ALTAIR radar electron densities through the cloud region to produce total electron content (TEC) values for direct comparison with the 2-D optical data. The absolute optical intensities are driven by twilight changes on the ground and at altitude, so for this analysis we use only the relative optical intensity between the radar beam location and the peak of the optical cloud. These relative optics-based intensities now need to be scaled with time to reflect the gradual decay of the cloud with time. If the ionization reaction proceeds to completion rapidly and recombination is slow, we would expect the total number of ions in the cloud to be roughly constant, and the decline in density to depend only on expansion of the cloud. The optical measurements showed the size of the cloud to increase very linearly with time in both observed dimensions. For this case of a fixed number of electrons and linear expansion in 3 dimensions, we would expect plasma densities in the cloud to have a  $t^{-3}$  temporal dependence, as the volume increases with the cube of the radial size. The optical intensities, and radar TEC values, however, have been integrated along the nearly vertical lines of sight, so the expansion in the vertical direction has no effect on the integrated density, and we expect the decline in TEC to have a dependence of  $t^{-2}$ .

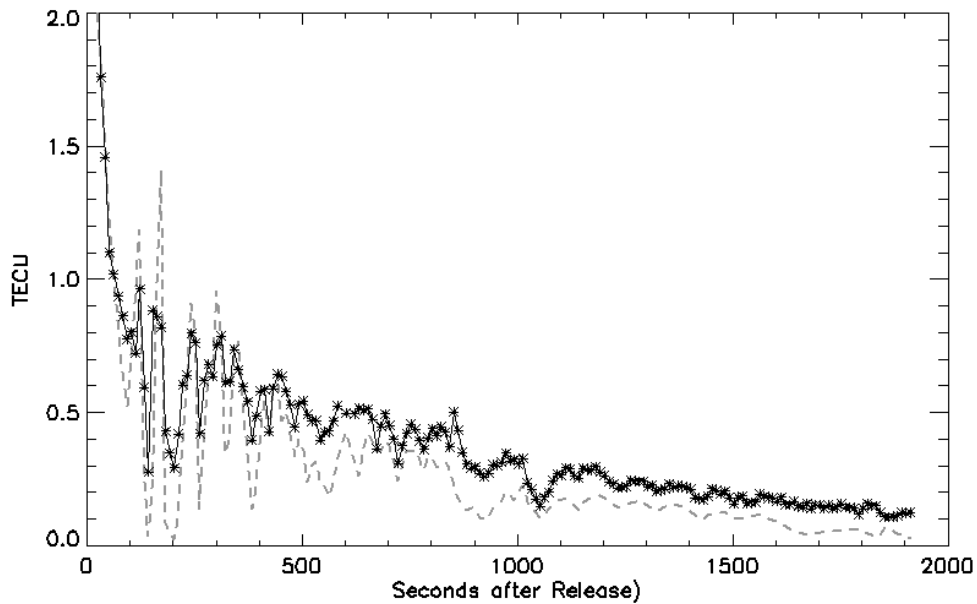


**Figure 3.** ALTAIR radar TEC measurements (black) compared with optics-derived relative intensities scaled by an overall temporal dependence of  $t^{-2}$  (gray) for MOSC Launch 2.

The gross features in this comparison, shown in Fig. 3, are clearly strongly correlated, even in the later period where the bumps are small. The peaks and valleys represent the scanning of the radar across the cloud rather than any complicated spatial structure in the cloud itself. The default  $t^{-2}$  scaling appears to be quite accurate up to about 500 sec, but underestimates the densities after that. The modulation of the curve from the radar scanning is also less severe in the actual radar TEC data (black) than in the optical model (gray) before 500 sec, possibly due to the finite beamwidth of the radar or the slightly oblique look angles here assumed to be strictly vertical. In any case, it is clear that the optical cloud model captures the primary plasma density structure of the cloud, even if the individual peaks from slices through the cloud are overrepresented in this version of the model.

### 3.3 COMPARISON WITH SOUNDER DATA

The ionosonde has a unique contribution to this modeling effort as it is inherently relatively insensitive to position but does pick out the maximum density of the isolated plasma clouds. So as long as the cloud is nearby, the ionosonde reflections will indicate the peak density within the cloud regardless of the cloud position. The ionosonde measurements therefore should provide an upper bound on the radar measurements, which only occasionally, if ever, cut through the exact center of the cloud.

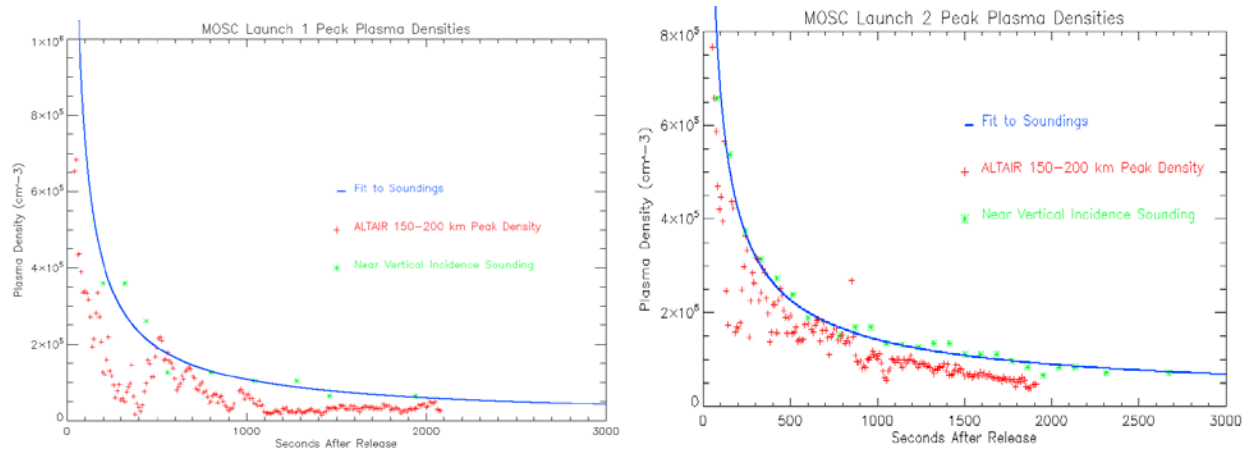


**Figure 4.** Comparison of ionosonde peak cloud densities (green) with ALTAIR radar measurements (red) for Launch 1 (left) and Launch 2 (right). The ALTAIR data points represent the maximum density along the radar line of sight between altitudes of 150 and 200 km, which span the cloud location and were well below the background F-region ionosphere. The blue line is a log-log fit to the ionosonde data points.

As Figure 4 above shows, this is indeed the case, and with very few exceptions, the peak density in the cloud at the radar beam location is at or below the sounder-measured density throughout both experiments. The log-log fits to the sounder data (blue lines) provide the overall temporal dependence for the peak densities,  $N_o(t)$ , and give numeric values of  $N_o(t) = 3.6 \times 10^7 t^{-0.84} \text{ cm}^{-3}$  for Launch 1 and  $N_o(t) = 1.5 \times 10^7 t^{-0.68} \text{ cm}^{-3}$  for the second launch. These numerical fits to the sounder density measurements now provide an opportunity to examine the assumptions introduced earlier of constant ion number and linear expansion with time.

#### 4. DISCUSSION

As we have seen, the optical measurements correlate well with radar data from the ALTAIR radar, when put into the proper coordinate system moving with the cloud, and assumptions based on constant total number of ions and observed linear expansion produce realistic temporal profiles for measurements. The most surprising aspect of these fits are the very small exponents, which are roughly  $-3/4$  and much smaller in magnitude than the  $-3$  exponent expected even for constant number of ions. This suggests that production may have been ongoing during the lifetime of the clouds. We note that theoretical treatments of artificial cloud expansion, in particular [Ma and Schunk, 1993] give a  $t^{-3/2}$  temporal dependence of peak density due to diffusion, which is much larger than our observational fit but much less than what would be expected from a linear expansion of the type observed in MOSC. Another possible mechanism that would produce a low exponent is flux-tube containment of plasma, which would essentially limit expansion to 1 dimension and give an exponent close to  $-1$  for a linear temporal dependence in 1 dimension. The good correlation between the radar data and optical model, however, rule this possibility out for the MOSC releases. If anything, the radar TEC data show *less* change in density scanning across the cloud than the optical model does, which suggests that the actual plasma cloud may be somewhat larger than the optical cloud.

The limited asymmetry of the optical clouds relative to the magnetic field ( $\sim 2:1$  elongation for Launch 2) suggests that much of the material remained neutral for an extended period. This could provide a widespread source for additional photo- or chemical ionization to occur throughout the

experiment and compensate for the decrease in density resulting from the observed expansion. Although both MOSC launches had identical payloads, the peak densities from Launch 1 were considerably lower than for Launch 2, and it was suggested that one of the two canisters may have failed to operate properly. Our empirical fit to the peak density, however, gives a higher overall density coefficient for Launch 1 than Launch 2, with the observed densities being lower due to the larger negative exponent. While extrapolations of these relationships back to very early times are not useful, as the cloud evolution was non-linear at the early stages, the overall trend suggests that faster decay, rather than lower initial density, was the cause of the lower densities from Launch 1. This fits with the more active conditions for Launch 1, the later launch time relative to sunset, and lower altitude, all of which resulted in lower solar zenith angles and an earlier terminator crossing than Launch 2, where the earlier solar local time and higher altitude provided for stronger solar illumination over a longer period of time.

## **5. CONCLUSIONS**

We have developed an initial empirical model of samarium cloud position, size, shape, and density for the MOSC releases carried out at Kwajalein in May 2013 based on all-sky imager, ALTAIR radar, and near-vertical-incidence ionospheric soundings. The optics-based measurements correlate well with radar density measurements integrated along lines of sight into 2-D total electron content measurements, and are consistent with a  $t^{-2}$  temporal dependence applicable to a constant number of electrons and linear expansion of the clouds. Peak density measurements from the sounder, however, indicate a much slower rate of decrease in density, with exponents near -0.75. This suggests ongoing ionization during the observation period which partially filled in the additional volume created by the observed linear expansion of the clouds. The empirical model is now being applied for detailed modeling of RF propagation and electrodynamic impacts on the background ionosphere.

## **ACKNOWLEDGEMENTS**

The MOSC experiment was supported by the Department of Defense Space Test Program. Payload integration and launch were provided by the NASA Sounding Rocket Program. Analysis at AFRL was supported by the Air Force Office of Scientific Research. We thank R. Todd Parris and Y.-J. Su for configuring and operating the ionosonde at Roi Namur.

## **REFERENCES**

Ma, T.-Z., and R. W. Schunk (1993), Ionization and Expansion of Barium Clouds in the Ionosphere, *J. Geophys. Res.*, 98(A1), 323-336.